

# TCDiff++: An End-to-end Trajectory-Controllable Diffusion Model for Harmonious Music-Driven Group Choreography

Yubin Dai<sup>1,2†</sup>, Wanlu Zhu<sup>1†</sup>, Ronghui Li<sup>2</sup>, Xiu Li<sup>2</sup>, Zhenyu Zhang<sup>3\*</sup>, Jun Li<sup>1\*</sup>,  
Jian Yang<sup>1\*</sup>

<sup>1</sup>PCA Lab, Key Lab of Intelligent Perception and Systems for High-Dimensional Information of Ministry of Education, School of Computer Science and Engineering, Nanjing University of Science and Technology, Nanjing, China.

<sup>2</sup>Shenzhen International Graduate School, Tsinghua University, Shenzhen, China.

<sup>3</sup>Nanjing University, Suzhou, China.

\*Corresponding author(s). E-mail(s): [zhenyuzhang@nju.edu.cn](mailto:zhenyuzhang@nju.edu.cn); [junli@njust.edu.cn](mailto:junli@njust.edu.cn); [csjyang@njust.edu.cn](mailto:csjyang@njust.edu.cn);

Contributing authors: [daiy@njust.edu.cn](mailto:daiy@njust.edu.cn); [wanluzhu@njust.edu.cn](mailto:wanluzhu@njust.edu.cn); [lrh22@mails.tsinghua.edu.cn](mailto:lrh22@mails.tsinghua.edu.cn); [li.xiu@sz.tsinghua.edu.cn](mailto:li.xiu@sz.tsinghua.edu.cn);

<sup>†</sup>Equal contribution

## Abstract

Music-driven dance generation has garnered significant attention due to its wide range of industrial applications, particularly in the creation of group choreography. During the group dance generation process, however, most existing methods still face three primary issues: *multi-dancer collisions*, *single-dancer foot sliding* and *abrupt swapping in the generation of long group dance*. In this paper, we propose TCDiff++, a music-driven end-to-end framework designed to generate harmonious group dance. Specifically, to mitigate multi-dancer collisions, we utilize a dancer positioning embedding to better maintain the relative positioning among dancers. Additionally, we incorporate a distance-consistency loss to ensure that inter-dancer distances remain within plausible ranges. To address the issue of single-dancer foot sliding, we introduce a swap mode embedding to indicate dancer swapping patterns and design a Footwork Adaptor to refine raw motion, thereby minimizing foot sliding. For long group dance generation, we present a long group diffusion sampling strategy that reduces abrupt position shifts by injecting positional information into the noisy input. Furthermore, we integrate a Sequence Decoder layer to enhance the model’s ability to selectively process long sequences. Extensive experiments demonstrate that our TCDiff++ achieves state-of-the-art performance, particularly in long-duration scenarios, ensuring high-quality and coherent group dance generation. [Project Page](#).

**Keywords:** Music-driven Dance Generation, Group Choreography, Motion Generation, Diffusion Model

## 1 Introduction

As one of the most expressive forms of art, dance profoundly impacts cultural, cinematic, and

academic domains ([Artemyeva and Moshenska, 2018](#); [Lee et al, 2021](#); [Yao et al, 2023](#); [Xue et al, 2024](#)). This influence stems from the intricate process of choreography, where movement

and music converge, synchronizing rhythm and structure to produce a harmonious and cohesive artistic expression. Traditionally, choreography has been a labor-intensive endeavor, spurring the development of automated models for dance creation. Consequently, music-driven choreography, initially centered on solo dancers (Li et al, 2021; Tseng et al, 2023a; Li et al, 2023), has garnered considerable attention. With the growing demand for more immersive and interactive experiences, the focus has changed to multi-person choreography (Yao et al, 2023). This evolution underscores the dual challenge of achieving synchronization in group movements while maintaining individuality within the ensemble, thereby enhancing the audience’s engagement and creating a more dynamic experience (Schwartz, 1998). Despite early recognition and exploration (Yao et al, 2023; Le et al, 2023b,a; Yang et al, 2024), these approaches continue to face three significant problems:

**Multi-dancer collisions.** Many group choreography frameworks (Le et al, 2023b,a; Yao et al, 2023) construct model inputs by concatenating the movements and coordinates of each dancer. However, this approach introduces a notable imbalance, as movements typically span over 100 dimensions, while coordinates are limited to just three. In group choreography, while dancers’ positions can vary considerably, their movements often exhibit substantial similarity. For instance, more than 80% of the movements in the AIOZ-GDance dataset (Le et al, 2023b) are alike. This results in *dancer ambiguity*, making it challenging for models to distinguish between individual dancers, which frequently leads to collisions, as illustrated in Figure 1. In our previous work (Dai et al, 2025), we introduced the Dance-Trajectory Navigator (DTN), which focuses on key positional coordinates and uses a distance-consistency loss to prevent collisions. Although this approach reduces ambiguity, it still struggles to manage highly dynamic group interactions, particularly in scenarios involving numerous dancers and complex movements, often resulting in misalignment or collisions.

**Single-dancer foot sliding.** Foot sliding occurs when a dancer’s feet appear to glide across the ground while the upper body maintains proper movement, as illustrated in Figure 1. This issue often arises from difficulties in accurately modeling the relationship between global trajectory and

local body rotations (Yang et al, 2023). In multi-person choreography, dancer ambiguity makes this alignment even more difficult, further complicating footwork synchronization with movement.

**Long group dance generation.** Existing models (Le et al, 2023b,a; Yang et al, 2024; Dai et al, 2025) have demonstrated the ability to generate group dance movements lasting several seconds. Unfortunately, a full group dance performance synchronized with music typically spans several minutes and, in the case of musicals, can extend to hours. This disparity highlights a critical gap in current capabilities, underscoring the urgent need for methods capable of generating long-duration group dance motions. To tackle the challenge of long-duration generation, current methods first generate partially overlapping segments and then smooth the overlapping regions when stitching them together to form a coherent sequence. Consequently, ensuring consistency in these overlapping regions is essential for achieving seamless and continuous results.

Drawing inspiration from the solo-dance model (Tseng et al, 2023a), diffusion-based methods (Le et al, 2023a; Dai et al, 2025) enforce this consistency during the sampling stage. However, group dance introduces an additional layer of complexity: it allows for *dancer swapping*, where any two dancers can exchange positions while maintaining a reasonable formation. This flexibility introduces a contradiction when merging segments, as dancers’ positions may vary across different sampling batches, resulting in positional inconsistencies. As a result, after stitching the segments, the same dancer may appear in discontinuous positions, causing abrupt and visually jarring shifts. These unnatural transitions significantly degrade the visual quality of long-duration group dance generation, posing a major challenge for achieving realistic and coherent performances.

A preliminary version of this work is the TCDiff (Trajectory-Controllable Diffusion) (Dai et al, 2025), which was published in AAAI 2025. TCDiff proposes a two-stage framework that first uses a Dance-Trajectory Navigator (DTN) to predict dancers’ coordinates, followed by a Trajectory-Specialist Diffusion (TSD) that generates movements based on these coordinates. The DTN focuses on learning coordinates with significant variations, while the TSD captures motion features with high similarity. This separation ensures

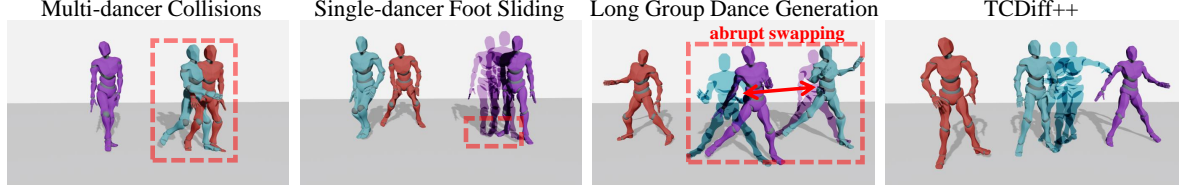


**Fig. 1** Visualizations of three key issues in baseline models: multi-dancer collisions (Dai et al, 2025), single-dancer foot sliding (Yang et al, 2024) and long group dance generation (Le et al, 2023a) where the blue man and the purple man suddenly swapped positions. In contrast, our approach eliminates these issues, delivering superior visual aesthetics.

distinct trajectory coordinates, effectively preventing dancer collisions.

However, the decoupled nature of this two-stage process separates the modeling of footwork and movement, often resulting in disjointed actions and displacements. Additionally, the disregard for movement dynamics introduces uncertainties in trajectory generation. These uncertainties accumulate over time, particularly in long group dance sequences, leading to performance degradation such as sharp oscillations. As a result, TCDiff is ill-suited for long-duration scenarios. Furthermore, the model architecture lacks selectivity, which exacerbates its performance decline in extended sequences. The two-stage design also limits its potential to inform subsequent end-to-end models, thereby restricting TCDiff’s broader applicability and impact.

To address the aforementioned issues, we upgrade the preliminary conference version (Dai et al, 2025) into a fully end-to-end model. This end-to-end design not only produces more coherent body movements and positions but also significantly enhances performance in long-duration scenarios. Specifically, **to mitigate multi-dancer collisions**, we newly develop a Dancer Positioning Embedding (DPE) that incorporates spatial information by encoding features based on the relative left-right positioning of dancers. The DPE enables the model to better preserve dancer positioning patterns and effectively prevent collisions. Additionally, while the distance-consistency loss was originally applied only within the DTN module, in this work, we apply it to the entire end-to-end model to enforce global consistency. The end-to-end application of the distance-consistency loss leads to more effective control of the spacing between generated positions. To further address dancer ambiguity, we implement a simple yet effective Fusion Projection module (FP) to enhance the distinction between

dancers in high-dimensional space, effectively mitigating dancer ambiguity. **For single-dancer foot sliding**, we newly integrate swap mode information, which specifies the start and end positions of dancers, thereby reducing spatial uncertainty caused by swap actions during generation. This enriched spatial information helps mitigate irregular foot sliding. Moreover, we refine the Footwork Adaptor plugin in TCDiff to directly adjust the generated results, improving the consistency between footwork and motion. **To facilitate long dance generation**, we remove the DTN module, which tends to cause oscillations due to spatial uncertainties in long-duration generation. To further reduce abrupt position shifts caused by dancer swapping, we propose the long group diffusion sampling strategy. This method constrains the input noise and incorporates positional priors, improving position consistency and minimizing sudden swaps. Additionally, we introduce the Sequence Decoder to strengthen the model’s sequence selection capability, further enhancing its performance in long-duration generation scenarios. In summary, our main contributions are:

- To prevent multi-dancer collisions, we introduce a dancer positioning embedding to maintain relative positions and adapt the distance-consistency loss for end-to-end models, ensuring reasonable spacing. Additionally, a simple yet effective FP module is used to efficiently reduce dancer ambiguity.
- For single-dancer foot sliding, we newly integrate swap mode information to reduce spatial uncertainty and enhance the Footwork Adaptor, improving footwork-motion consistency in the end-to-end model’s outputs.
- To facilitate long dance generation, our end-to-end architecture removes the DTN module to avoid oscillations from spatial uncertainties in long dance generation. We propose a long group

diffusion sampling strategy, injecting positional information to reduce abrupt swapping, and introduce a Sequence Decoder layer to improve sequence selection for long-duration generation.

- We propose TCDiff++, an end-to-end group dance generation model that surpasses the two-stage version in producing coherent body movements and handling long sequences. This widely applicable design also provides insights for future end-to-end models. Extensive experiments and analyses confirm the superiority of our approach over existing methods.

## 2 Related Work

### 2.1 Single-dancer Generation

Group dance generation extends single-dancer generation, but directly applying single-dancer methods to group dance presents significant challenges (Joshi and Chakrabarty, 2021). Early motion retrieval methods (Kovar and Gleicher, 2002; Fan et al, 2011; Offi et al, 2011; Lee et al, 2013) often produce deformed actions. Recent approaches use large datasets (Lee et al, 2019; Huang et al, 2020; Valle-Pérez et al, 2021; Li et al, 2021, 2023; Han et al, 2023) and deep learning techniques, such as auto-regressive models (Alemi et al, 2017; Yalta et al, 2019; Ahn et al, 2020; Li et al, 2024c; Siyao et al, 2022) and generative models (Kim et al, 2022; Tseng et al, 2023a; Li et al, 2024e,d; Zhou et al, 2023), to generate motions. Recently, diffusion-based models (Ho et al, 2020a; Sohl-Dickstein et al, 2015; Tseng et al, 2023a; Ren et al, 2025) have emerged, achieving state-of-the-art performance with high diversity and fidelity. Solo dance generation emphasizes realism, where artifacts like foot sliding are unacceptable (Yang et al, 2023). To address this, existing methods impose physical constraints through loss functions and foot contact labels (Zhang et al, 2021a, 2023; Tseng et al, 2023a; Li et al, 2024e).

Since music often lasts for several minutes, and some musicals extend for hours, improving performance in long-duration scenarios is crucial. To address long-duration generation, some work (Zhang et al, 2024; Li et al, 2024e) proposes a progressive generation approach, where dance segments rich in choreography information are generated first, followed by a second stage that completes the transitions between these segments. The

resulting segments are then concatenated to form a full-length dance sequence. However, single-dancer models often face issues with dancer ambiguity, arising from the severe similarity in dancer representations, result in multi-dancer collisions. In this paper, we address this issue by introducing a dancer positioning embedding, which incorporates relative left-right positioning information to aid spatial pattern learning. Furthermore, we directly apply the distance-consistency loss to the generated results, constraining the spacing between positions within a reasonable range.

### 2.2 Multi-dancer Generation

Multi-dancer generation is an emerging field in its early stages. To our knowledge, few studies (Yao et al, 2023; Le et al, 2023b,a; Yang et al, 2024; Le et al, 2024; Dai et al, 2025) have focused on scenarios with more than two dancers. Among them, GDanceR (Le et al, 2023b) and GCD (Le et al, 2023a) do not employ any specific structures to address motion representation imbalance, leading to dancer ambiguity. CoDancers (Yang et al, 2024) splits group motions into single-dancer motions to achieve scalability by incrementally adding dancers to the formation. As a result, this division causes the models to acquire only local information, leading to suboptimal group visual effects. TCDiff (Dai et al, 2025) is our previous version, a two-stage framework that first predicts dancers’ coordinates and then generates corresponding movements based on obtained coordinates. This separation preserves global formation features and ensures distinct trajectory coordinates, thus preventing dancer collisions caused by ambiguity. However, this two-stage generation process decouples footwork and movement modeling, making it prone to disjointed actions and displacements. Therefore, designing a model architecture that can both mitigate dancer ambiguity and simultaneously capture complete global and local information is in urgent need. In this paper, we upgrade the previous TCDiff to an end-to-end structure, enabling it to simultaneously capture global and local information. Furthermore, to mitigate dancer ambiguity, we modify the components from the original model and integrate new modules into the framework. These additions apply additional spatial constraints for further improvement.

## 2.3 Diffusion Model

In recent years, Diffusion Models (DM) (Ho et al, 2020b; Song et al, 2020) have demonstrated outstanding performance in the content generation domain (Bar-Tal et al, 2024; Wu et al, 2024; Xiong et al, 2024; Li et al, 2024b,a; Zhu et al, 2024). Compared to earlier generative models (Kingma, 2013; Goodfellow et al, 2020), such as Variational Auto-Encoders (VAE) (Kingma, 2013) and Generative Adversarial Networks (GAN) (Goodfellow et al, 2020), DMs offer significant advantages. Specifically, VAEs suffer from limited fidelity in learning complex, high-dimensional data distributions, while GANs are prone to mode collapse due to the challenges in balancing the adversarial relationship between generator and discriminator (Xue et al, 2024). In contrast, DMs leverage probabilistic inference chains to learn complex distribution and do not have adversarial relationships, enabling higher fidelity and more stable training. Similar to previous generative approaches, diffusion models are also capable of conditional generation. This ability is particularly important in motion generation, especially for human motion and dance synthesis (Liang et al, 2024; Dabral et al, 2023). In these tasks, conditional inputs, such as text (Wang et al, 2023; Zhou and Wang, 2023; Zhou et al, 2024), audio (Alexanderson et al, 2023; Tseng et al, 2023b) serve as crucial guidance, directing the model to generate the desired outcomes. However, dancer swapping introduces uncertainty during the diffusion sampling stage, leading to contradictory generation results. This contradiction leads to inconsistencies, as dancers’ positions vary across different sampling instances, resulting in abrupt swapping. To address this, we propose the long group diffusion sampling strategy, which constrains input noise and incorporates positional priors to enhance position consistency and reduce sudden swaps.

## 3 Background

### 3.1 Problem Definition

Given an input music sequence  $\mathcal{M} = \{\mathbf{m}_i\}_{i=1}^L$  with  $i = \{1, \dots, L\}$  indicates the index of the music frames, group choreography is to generate a corresponding group dance movement sequence

$\mathbf{x} = \{\mathbf{x}^{(i)}\}_{i=1}^L$ . Here,  $\mathbf{x}^{(i)} = \{\mathbf{x}^{(i),c}\}_{c=1}^C$ , where  $\mathbf{x}^{(i),c}$  is the generated pose of  $c$ -th dancer at  $i$ -frame.  $\mathbf{x}^c = \{\mathbf{x}^{(i),c}\}_{i=1}^L$  represents the movement sequence of the  $c$ -th dancer. For simplicity, we use  $\mathbf{x}_t$  to represent  $\{\mathbf{x}_t^{(i),c}\}$  at  $t$  step.

### 3.2 Motion and Music Features

The dancer’s motion is modeled using a 24-joint SMPL framework (Loper et al, 2023), with each joint’s pose  $\mathbf{d} \in \mathbb{R}^{24 \times 6=144}$  expressed in 6D rotation (Zhou et al, 2019). This model also includes binary contact indicators  $\mathbf{f} \in \mathbb{R}^4$  for the heels and toes, and a 3D root position  $\mathbf{p} \in \mathbb{R}^3$ , forming a complete motion descriptor  $\mathbf{x} = [\mathbf{f}, \mathbf{p}, \mathbf{d}] \in \mathbb{R}^{144+4+3=151}$ . This rotation-based approach enhances motion smoothness over traditional 3D keypoint methods (Zhang et al, 2021b; Zangir et al, 2021; Ma et al, 2023; Siyao et al, 2022). For audio analysis, we utilize the Librosa toolkit (McFee et al, 2015) to derive a 35-dimensional feature set  $\mathcal{M} \in \mathbb{R}^{35}$ , which includes an audio envelope, 20 MFCCs for spectral details, 12 chroma features for pitch, and binary indicators for beats and peaks, essential for aligning movements with audio rhythms.

### 3.3 Diffusion for Dance Generation

We utilize a diffusion framework (Ho et al, 2020a) to obtain dance sequence. The method constructs a Markov chain that progressively perturbs the original data  $\mathbf{x}_0$  toward a standard Gaussian distribution  $\mathbf{x}_T \sim \mathcal{N}(0, \mathbf{I})$  through  $T$  iterative noise injection stages. This forward process is defined as:

$$q(\mathbf{x}_t | \mathbf{x}_{t-1}) = \mathcal{N}(\sqrt{\alpha_t} \mathbf{x}_{t-1}, (1 - \alpha_t) \mathbf{I}), \quad (1)$$

where  $\alpha_t \in (0, 1)$  denotes a predefined decay coefficient sequence, and  $\mathbf{I}$  is the identity matrix. The reverse process aims to denoise  $\mathbf{x}_T$  back to  $\mathbf{x}_0$ . Since estimating  $q(\mathbf{x}_{t-1} | \mathbf{x}_t)$  is challenging, the network  $p_\theta$  is trained to approximate  $\mathbf{x}_0$ :

$$p_\theta(\mathbf{x}_{t-1} | \mathbf{x}_t) = \mathcal{N}(\mathbf{x}_{t-1}; \mu_\theta(\mathbf{x}_t, t), \Sigma_\theta(\mathbf{x}_t, t)). \quad (2)$$

To synthesize group dance motion sequences based on music rhythm, we extend the conditional diffusion framework. Given the music condition  $\mathcal{M}$  (Tseng et al, 2023a) and the dancer spatial



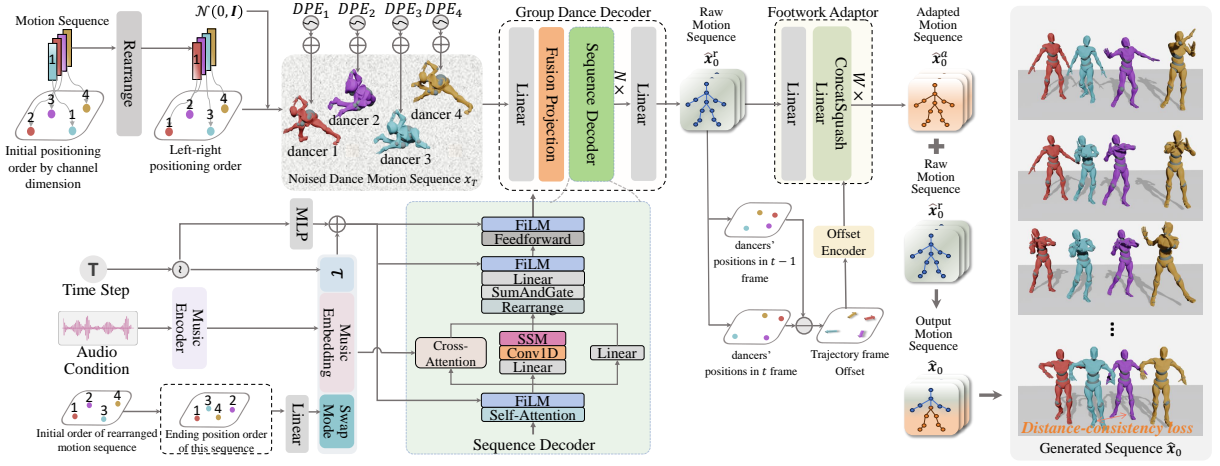


**Fig. 2** Our end-to-end TCDiff++ framework comprises two key components: the Group Dance Decoder (GDD) and the Footwork Adaptor (FA). The GDD initially generates a raw motion sequence  $\hat{\mathbf{x}}^r$  without trajectory overlap based on the given music. Subsequently, the FA refines the foot movements by leveraging the positional information of the raw motion, producing an adapted motion  $\hat{\mathbf{x}}_0^a$  with improved footstep actions to reduce foot sliding. Finally, the adapted footstep movements are incorporated into the raw motion, yielding a harmonious dance sequence  $\hat{\mathbf{x}}_0$  with stable footwork and less dancer collisions. Compared to the previous two-stage version, TCDiff++ requires only a single training stage, demonstrating better footwork-motion coherence performance.

condition swap mode  $S$ , the generation process reverses the forward diffusion trajectory through a learned denoising function  $D(\mathbf{x}_t, t, \mathcal{M}, S)$ , which estimates the clean motion  $\mathbf{x}$  at each time step  $t$ .

### 3.4 SSM Backbone

State Space Models (SSMs), such as structured state space sequence models (Gu et al, 2022a) and Mamba (Gu and Dao, 2023; Dao and Gu, 2024) are effective for long-sequence modeling due to their selective state transitions, linear computational complexity, and global receptive fields (Weng et al, 2024). They map an input  $x(t) \in \mathbb{R}$  to the output  $y(t) \in \mathbb{R}$  through a hidden state  $h(t) \in \mathbb{R}^N$ , described by a linear ordinary differential equation (ODE):

$$h'(t) = \mathbf{A}h(t) + \mathbf{B}x(t), \quad y(t) = \mathbf{C}h(t). \quad (3)$$

where  $N$  denotes the state size,  $\mathbf{A} \in \mathbb{R}^{N \times N}$  represents evolution parameter,  $\mathbf{B} \in \mathbb{R}^{N \times 1}$  and  $\mathbf{C} \in \mathbb{R}^{1 \times N}$  are projection parameters. For practical computation, the Mamba discretize the system using zero-order hold (ZOH), yielding discrete parameters  $\bar{\mathbf{A}} = \exp(\Delta\mathbf{A})$ ,  $\bar{\mathbf{B}} = (\Delta\mathbf{A})^{-1}(\exp(\Delta\mathbf{A}) - \mathbb{I})\Delta\mathbf{B}$ , where the input-dependent step size  $\Delta$  controls temporal granularity: small  $\Delta$  resolves fine details (e.g., rapid

motions), while large  $\Delta$  captures long-term transitions. The discretized SSM computes outputs via global convolution with a structured kernel  $\bar{\mathbf{K}}$ :

$$\bar{\mathbf{K}} = (\bar{\mathbf{C}}\bar{\mathbf{B}}, \bar{\mathbf{C}}\bar{\mathbf{A}}\bar{\mathbf{B}}, \dots, \bar{\mathbf{C}}\bar{\mathbf{A}}^{L-1}\bar{\mathbf{B}}), \quad (4)$$

$$\mathbf{y} = \mathbf{x} * \bar{\mathbf{K}},$$

where  $L$  is the input sequence length. This architecture improves the model’s selectivity, thereby enhancing its ability to process long sequences.

## 4 Methodology

In this section, we introduce TCDiff++, an end-to-end framework that can generate harmonious group dance movements according to the input music, as shown in Figure 2. Compared to the previous two-stage version, TCDiff++ requires only a single training stage to achieve harmonious dance generation, free from the spatial uncertainty caused by the process of generating motions and trajectories separately in the previous version. As a result, it demonstrates better footwork-motion coherence performance. TCDiff++ consists of a Group Dance Decoder (GDD) and a Footwork Adaptor (FA). The GDD first generates a raw motion sequence  $\hat{\mathbf{x}}^r$  without trajectory overlap

based on the music input. Then, the FA further modulates the foot movements using the raw motion’s positional information, generating adapted motion  $\hat{\mathbf{x}}^a$  with footstep actions that mitigate foot sliding. Finally, we integrate the footstep movements into the raw motion, resulting in a harmonious dance sequence  $\hat{\mathbf{x}}_0$  with grounded footwork and no dancer collisions.

#### 4.1 Group Dance Decoder

The Group Dance Decoder (GDD) reconstructs the input noisy dance motion sequence  $\mathbf{x}_T$  into a clean raw motion sequence  $\hat{\mathbf{x}}^r$ . GDD uses conditional generation to obtain  $\hat{\mathbf{x}}^r$ , incorporating not only the music condition  $\mathcal{M}$ , but also the diffusion time step  $T$  and the dancer spatial condition swap mode  $S$  to guide the generation of dancer motions. Namely, the generation of GDD, denoted as  $D(\cdot)$ , executes a reverse diffusion process by estimating  $D(\mathbf{x}_T, T, \mathcal{M}, S) \approx \hat{\mathbf{x}}^r$ . To be more specific, GDD first incorporates the Dance Positioning Embedding (DPE) into the input features to enhance spatial representation. The Fusion Projection then processes the representation to reduce dancer ambiguity. Next, the Sequence Decoder enhances feature extraction through sequence selection, producing the final raw motion  $\hat{\mathbf{x}}^r$ . We provide a detailed introduction to the modules of GDD in the following sections, starting with the Dance Positioning Embedding (DPE).

##### Dance Positioning Embedding (DPE).

We add the DPE to the input features to incorporate spatial information of the dancers, as shown in Figure 2. We find that dancers often display well-defined spatial relationships, such as maintaining a fixed left-right positional order to ensure no occlusion. Maintaining this positional information also helps alleviate dancer ambiguity and reduces the collisions. Based on the above findings, we designed the DPE to integrate additional spatial information into the features, helping to mitigate collisions. To be more specific, let the initial ground-truth motion sequences of  $C$  dancers be denoted as  $\{\mathbf{x}^C\}_{c=1}^C$ , where each dancer has a x-axis position coordinate  $p_c^{x-axis} \in \mathbb{R}$ . These sequences are reordered from left to right based on positional coordinates using a permutation operator  $\sigma(\cdot)$  to ensure monotonicity.

$$\sigma = \text{argsort}(p_1^{x-axis}, p_2^{x-axis}, \dots, p_C^{x-axis}), \quad (5)$$

$$\text{where, } p_{\sigma(1)}^{x-axis} \leq p_{\sigma(2)}^{x-axis} \leq \dots \leq p_{\sigma(N)}^{x-axis}. \quad (6)$$

This yields the sorted sequence

$$\mathbf{x}^{sorted} = \left\{ \mathbf{x}^{\sigma(c)} \right\}_{c=1}^C. \quad (7)$$

Next, the diffusion forward process is applied to  $\mathbf{x}^{sorted}$  to inject Gaussian noise, resulting in the noisy input  $\mathbf{x}_T^{sorted}$ . Finally, a dance position embedding  $\mathbf{DPE}$  is incorporated into each noisy sequence.

$$\mathbf{x}_T = \mathbf{DPE} + \mathbf{x}_T^{sorted}. \quad (8)$$

Here,  $\mathbf{DPE} \in \mathbb{R}^C$  is a set of positional embeddings, which is automatically broadcasted to  $\mathbf{DPE}' \in \mathbb{R}^{C \times L \times d}$  during addition. Then, we input  $\mathbf{x}_T$  into the Fusion Projection for further processing.

**Fusion Projection (FP).** FP increases the features to a high-dimensional space to amplify differences between dancers, thereby reducing dancer ambiguity. The FP module is designed under the principle that data in high-dimensional feature spaces can be more easily differentiated. To amplify the differences between dancers in this space, the FP module increases the input dimensionality by stacking the features of all dancers, as shown in Figure 3. To be more specific, given an input feature tensor  $\mathbf{x} \in \mathbb{R}^{C \times L \times d}$  with  $C$  channels (also the number of dancers),  $L$  frames, and hidden dimension  $d$ . We first concatenate the channel-wise features across all frames to form a reshaped tensor  $\mathbf{x}' \in \mathbb{R}^{L \times (C \times d)}$ . These high-dimensional features are then mapped through a Multi-Layer Perceptron (MLP), producing latent space feature vectors for all dancers. Dancer-specific features are obtained by rearranging these vectors. Unlike naive projection that maps a single dancer’s features with an MLP, this approach maps the features of all dancers simultaneously, using a higher-dimensional space. This enhances the model’s ability to capture differences at the group level in a higher-dimensional space, rather than at the individual level, effectively alleviating dancer ambiguity. Evidence for this is provided in the ablation study.

**Sequence Decoder (SD).** The SD enhances the model’s ability to selectively focus on long-duration information, utilizing the SSM architecture to improve selection in sequential data.

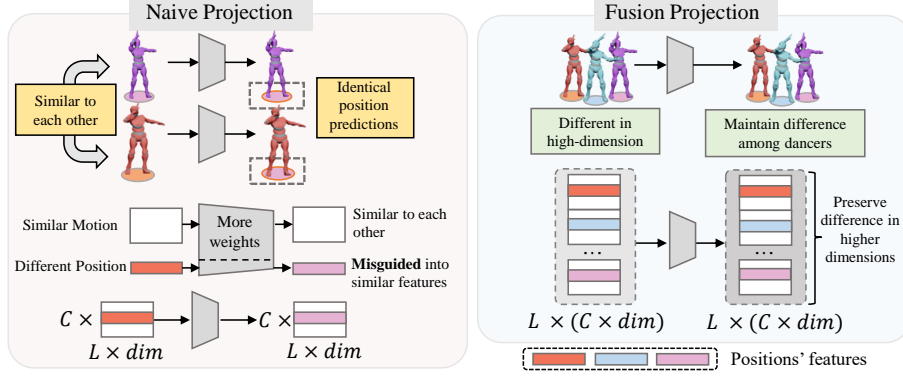


**Fig. 3** Our Fusion Projection (FP) module addresses the issue of dancer ambiguity. Imbalanced feature representations can cause positions to be misinterpreted as similar, leading to identical predictions. The FP module increases input dimensionality to enhance dancer differentiation, preserving positional differences and reducing collisions.

Specifically, the motion feature is first processed through self-attention for localized fine-grained modeling, followed by the SSM (Gu and Dao, 2023; Dao and Gu, 2024) for feature selection. We employ Cross-Attention to incorporate conditioning into the motion feature processing, while timestep information  $T$ , music conditioning  $\mathcal{M}$ , and dancer spatial condition swap mode  $S$  are concatenated and injected into Feature-wise Linear Modulation (FiLM) (Perez et al, 2018) to enhance the incorporation of conditional information.

The *swap mode*  $S$  is an embedding derived from a sequence of numbers, representing the left-to-right positional order of the dancers in the final frame. This positional information comes from the left-to-right order of the final positions in the sorted sequence  $\mathbf{x}^{sorted}$ . The indices of this order are mapped through a linear transformation to generate the final swap mode  $S$ . Swap mode adds positional information, helping reduce spatial uncertainty caused by the dancer swapping during generation.

## 4.2 Footwork Adaptor

Since positional changes are mainly caused by footwork, our Footwork Adaptor (FA) module exclusively adjusts the dancers' lower body movements rather than the whole body motion. Unlike the previous two-stage version, our end-to-end TCDiff++ does not have access to clean dancer trajectory coordinates in advance for conditional generation and trajectory modulation. To address this, we use the raw motion  $\hat{\mathbf{x}}^r$  generated by GDD as a substitute, extracting its trajectory

coordinates as conditions. We then employ FA to refine footwork, obtaining the adapted motion  $\hat{\mathbf{x}}^a$ , thereby reducing foot sliding occurrences. To be specific, the raw motion sequence generated by GDD,  $\hat{\mathbf{x}}^r = [\mathbf{f}^r, \mathbf{p}^r, \mathbf{d}^r]$ , includes the dancer's position data  $\mathbf{p}^r$ . We extract the coordinates and compute the frame-wise velocity by subtracting adjacent frames:

$$\mathcal{V} = \{\mathbf{p}_i^r - \mathbf{p}_{i-1}^r\}_1^L. \quad (9)$$

This velocity conditions the Footwork Adaptor module  $FA(\cdot)$  for correction, ultimately yielding the adapted motion  $\hat{\mathbf{x}}_0^a$ , as formulated below:

$$\hat{\mathbf{x}}^a = FA(\hat{\mathbf{x}}^r, \mathcal{V}). \quad (10)$$

Specifically, the Footwork Adaptor  $FA(\cdot)$  consists of a linear layer and a ConcatSquashLinear layer, as shown in Figure 2. This design has been proven effective in various coordinate prediction domains (Gu et al, 2022b; Luo and Hu, 2021). Since positional changes are predominantly driven by footwork, we replace the footwork-related motions to the adopted version to obtain the final output. Specifically, we use the footwork-related motions from the adapted motion  $\hat{\mathbf{x}}^a$  while preserving the expressive upper-body actions from the raw motion  $\hat{\mathbf{x}}^r$ , yielding the final generated result. Therefore, we split  $\hat{\mathbf{x}}^r$  and  $\hat{\mathbf{x}}^a$  into upper and lower body components. In other words,  $\hat{\mathbf{x}}^r = \{\hat{\mathbf{x}}_{upper}^r, \hat{\mathbf{x}}_{lower}^r\}$  and  $\hat{\mathbf{x}}^a = \{\hat{\mathbf{x}}_{upper}^a, \hat{\mathbf{x}}_{lower}^a\}$ .

We then take the upper-body part from  $\hat{\mathbf{x}}^r$  and the lower-body part from  $\hat{\mathbf{x}}^a$ , which contains the



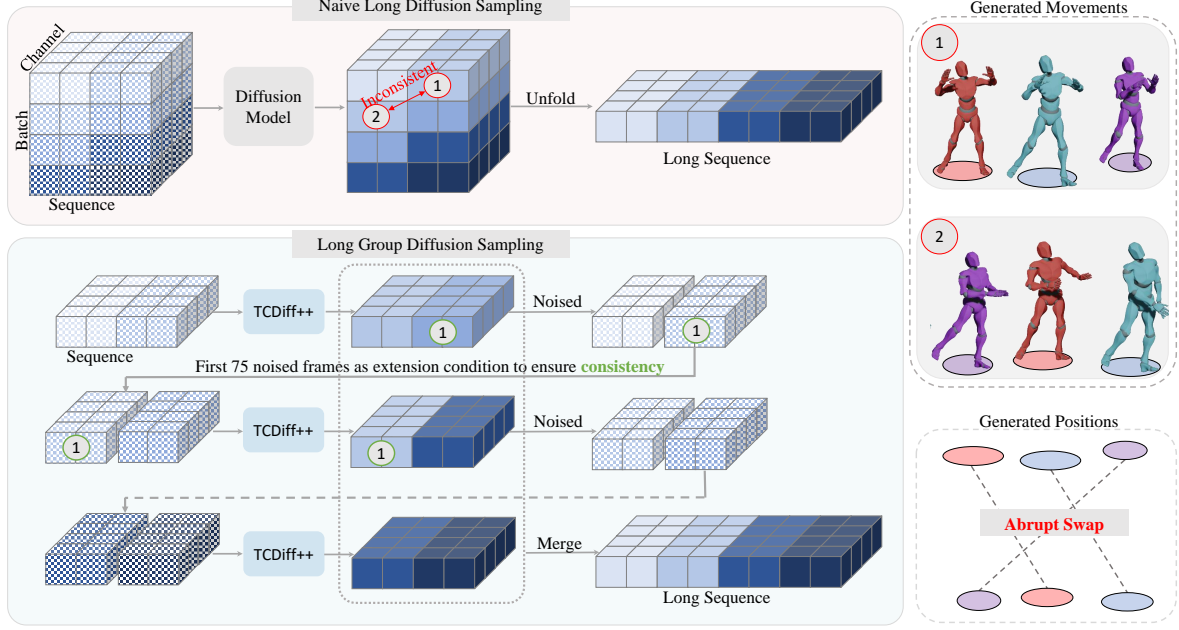


**Fig. 4** Our Long Group Diffusion Sampling (LGDS) method initially generates segments with partial overlap, which are then merged to form a complete sequence. Unlike naive sampling, LGDS enforces consistency during the input phase rather than the sampling phase. This approach reduces randomness and ensures cleaner positional information during generation, thereby reducing abrupt swap.

detailed footwork, to form the final output:

$$\hat{\mathbf{x}}_0 = \hat{\mathbf{x}}_{\text{upper}}^r \oplus \hat{\mathbf{x}}_{\text{lower}}^a \quad (11)$$

This approach allows the FA module to effectively combine footwork with positional information, thus refining the footwork in the raw sequence. We show our effectiveness in Section 5.4.

### 4.3 Training Loss

Our TCDiff++ integrates the losses from the previous two-stage framework into a single framework, enabling more efficient end-to-end training. Specifically, the simple loss  $\mathcal{L}_{\text{simple}}$  of the diffusion model is used to ensure that the reconstructed results are close to the ground truth:

$$\mathcal{L}_{\text{simple}} = \mathbb{E}_{x,t} [\|\mathbf{x}_0 - D(\mathbf{x}_T, T, \mathcal{M}, S)\|_2^2], \quad (12)$$

We adopt the joint velocity loss  $\mathcal{L}_{\text{vel}}$  to ensure motion continuity between frames, the foot contact loss  $\mathcal{L}_{\text{con}}$  to further constrain foot-ground contact, and the Forward-Kinematic loss  $\mathcal{L}_{\text{FK}}$  to maintain the spatial consistency of the dancer's skeletons:

$$\mathcal{L}_{\text{FK}} = \frac{1}{N} \sum_{i=1}^N \|FK(\mathbf{x}_0^{(i)}) - FK(\hat{\mathbf{x}}_0^{(i)})\|_2^2, \quad (13)$$

$$\mathcal{L}_{\text{vel}} = \frac{1}{N-1} \sum_{i=1}^{N-1} \left\| (\mathbf{x}_0^{(i+1)} - \mathbf{x}_0^{(i)}) - (\hat{\mathbf{x}}_0^{(i+1)} - \hat{\mathbf{x}}_0^{(i)}) \right\|_2^2, \quad (14)$$

$$\mathcal{L}_{\text{con}} = \frac{1}{N-1} \sum_{i=1}^{N-1} \left\| (FK(\hat{\mathbf{x}}_0^{(i+1)}) - FK(\hat{\mathbf{x}}_0^{(i)})) \cdot \hat{\mathbf{d}}^{(i)} \right\|_2^2. \quad (15)$$

Here,  $FK(\cdot)$  is the forward kinematic function that calculates the positions of joints given the 6D rotation motion. Further, we integrate our distance-consistency loss  $\mathcal{L}_D$ :

$$\Delta \mathbf{p}^{(w),ij} = (\mathbf{p}^{(w),i} - \mathbf{p}^{(w),j}) - (\hat{\mathbf{p}}^{(w),i} - \hat{\mathbf{p}}^{(w),j}), \quad (16)$$

$$\mathcal{L}_D = \frac{1}{C-1} \sum_{w=1}^L \binom{C}{2}_{ij} \|\Delta \mathbf{p}^{(w),ij}\|_2^2, \quad (17)$$

which ensures that the spacing among dancers is within an appropriate range. The overall objective of our proposed TCDiff++ is:

$$\mathcal{L}_{\text{TCDiff++}} = \lambda_{\text{sim}} \mathcal{L}_{\text{simple}} + \lambda_{\text{FK}} \mathcal{L}_{\text{FK}} + \lambda_{\text{vel}} \mathcal{L}_{\text{vel}} + \lambda_{\text{con}} \mathcal{L}_{\text{con}} + \lambda_D \mathcal{L}_D \quad (18)$$

where  $\lambda_{\text{sim}}$ ,  $\lambda_{\text{FK}}$ ,  $\lambda_{\text{vel}}$ ,  $\lambda_{\text{con}}$ , and  $\lambda_D$  are the balanced hyper-parameters.

### 4.4 Long Group Diffusion Sampling

We initially generate segments with partial overlap and subsequently merge them to construct a

complete sequence. Due to dancer swapping in group dance, dancers’ positions can vary across different sampling epochs. This makes it difficult to ensure consistency during the sampling stage, resulting in inconsistent positions during long-term generation. Based on this finding, we propose Long Group Diffusion Sampling (LGDS) strategy to eliminate the uncertainty during sampling, resulting in more consistent generation. LGDS can autoregressively extend short sequences by using the generated results as conditions, as illustrated in Figure 4. This constrains the generation consistency during the input phase, rather than the sampling phase. To be more specific, for a sequence of 150 frames, Instead of directly inputting random noise, we first sample a short clean segment  $\hat{\mathbf{x}}_0^{[0:150]} = \{\hat{\mathbf{x}}_t^{(1)}, \dots, \hat{\mathbf{x}}_t^{(75)}, \dots, \hat{\mathbf{x}}_t^{(150)}\}$ , then add noise to obtain noised data  $\hat{\mathbf{x}}_T^{[0:150]}$ . This noise data is used as input for the next step, recursively extending the sequence. The input can be represented as

$$\hat{\mathbf{z}}_T^{[75:225]} = [\hat{\mathbf{x}}_T^{[75:150]}, \mathbf{z}_T^{[151:225]}], \quad (19)$$

where  $[\cdot, \cdot]$  denotes the concatenation operation,  $\mathbf{z}_T^{[151:225]}$  is a random noise, and  $\hat{\mathbf{z}}_T^{[75:225]}$  is the final input noise. Compared to the existing method, this approach, which constrains the input noise, introduces less randomness and provides cleaner positional constraints during generation, thus effectively improving the consistency of the transitions in long-term generation. We provide further analysis in the ablation study section, demonstrating the effectiveness of our approach.

## 5 Experiments

### 5.1 Experimental Settings

**Implementation Details.** Our model employs a diffusion-based architecture comprising the Group Dance Decoder (GDD) and the Footwork Adaptor (FA). We set the hidden size of all components in our framework to  $d = 512$ . In GDD, a linear layer first transforms the 151-dimensional input motion into a 512-dimensional hidden representation. This representation is then processed by the Fusion Projection, which consists of a three-layer MLP with ReLU activation. Next, the Sequence Decoder, composed of  $M = 8$  stacked layers

and equipped with eight attention heads, extracts sequential information from the data. Finally, an output linear layer maps the hidden features back to 151-dimensional raw motion data. For footwork modulation, we construct the FA using  $W = 3$  stacked Concat Squash Linear layers. We set the weighting coefficients as follows:  $\lambda_D = \lambda_{\text{Sim}} = 0.636$ ,  $\lambda_{\text{vel}} = 2.964$ ,  $\lambda_{\text{FK}} = 0.646$ , and  $\lambda_{\text{con}} = 10.942$ . We used batch sizes of 72, 53, 40, and 23 per GPU for 2, 3, 4, and 5 dancers, respectively. We using Adam for optimization with a learning rate of  $5 \times 10^{-5}$ .

**Dataset.** The open-source AIOZ-GDance dataset (Le et al, 2023b) provides 16.7 hours of 3D multi-dancer motion that capture data for group dance performances, synchronized with musical accompaniment. Each video lasts 15 to 60 seconds and is decoded at 30 FPS. It features over 4,000 performers, ensuring diversity in motion and auditory content. Following the protocol in (Le et al, 2023b), videos are partitioned into training (80%), validation (10%), and test (10%) sets.

**Compared methods.** We evaluate TCDiff++ against four publicly available group dance generation baselines:

- GCD (Le et al, 2023a) leverages contrastive diffusion for controllable group dance generation, balancing diversity and coherence via user-guided adjustments.
- CoDancers (Yang et al, 2024) decomposes group dance into individual solo dances, generating dancers sequentially and ultimately assembling them into a cohesive group performance.
- TCDiff (Dai et al, 2025) is our previous version, a two-stage model that first generates dancers’ trajectories and then their corresponding movements, enabling collision-free results in short-duration scenarios.
- We adapt EDGE (Tseng et al, 2023a) for further comparison, a leading single-dancer model, by training it on the AIOZ-GDance dataset to benchmark its generalization to group settings.

To the best of our knowledge, these represent all the available group dance generation models capable of producing choreography for two or more dancers. Our previous version, TCDiff, is the current state-of-the-art method. In this paper, we adopt an end-to-end design to enhance the consistency of footwork motion and improve its



**Fig. 5** Visual comparison with Baselines. Baselines often cause collisions (highlighted in the red box) during exchanges.

performance in long-term generation, achieving superior results.

**Metrics.** We evaluate our model using metrics for both multi-dancer and single-dancer assessments. For multi-dancer evaluation (Le et al, 2023b), (1) Group Motion Realism (GMR) measures group formation feature similarity using the Frechet Inception Distance (FID). (2) Group Motion Correlation (GMC) assesses coherence by calculating the cross-correlation between generated dancers. (3) The Trajectory Intersection Frequency (TIF) evaluates how often dancers collide during movement. For single-dancer evaluation, (4) the Frechet Inception Distance (FID) (Li et al, 2021; Heusel et al, 2017) quantifies the similarity between individual dances and ground-truth dances. (5) Generation Diversity (Div) (Li et al, 2021; Huang et al, 2020) measures the variety of dance movements using kinematic features. (6) Motion-Music Consistency (MMC) (Li et al, 2021) examines how well the generated dances synchronize with the music’s rhythm. (7) The Physical Foot Contact (PFC) (Tseng et al, 2023a) score evaluates the physical plausibility of footwork by analyzing the relationship between the center of mass and foot velocity.

## 5.2 Qualitative Visual Comparison

**Baseline visual comparison.** Figure 5 illustrates the performance comparison between our model and the baselines. The results indicate that the single-dancer model EDGE is affected by the dancer ambiguity phenomenon, leading to dancer collisions. This demonstrates the difficulty of directly applying single-dancer models to multi-dancer generation scenarios. The group dance model GCD utilizes global attention mechanisms to capture dancer interactions. However, it neglects positional differences, resulting in multi-dancer collisions. CoDancers produces unreasonable initial positions due to incomplete group information, resulting in severe overlaps. TCDiff addresses the trajectory overlap issue caused by dancer ambiguity through a two-stage generation approach. However, this two-stage process decouples trajectory modeling from body modeling, resulting in suboptimal performance. This decoupling causes the dancer’s coordinates to gradually converge, ultimately leading to collisions. In contrast, TCDiff++ employs an end-to-end generation approach, leveraging the design of internal modules to enhance the distinction between spatial

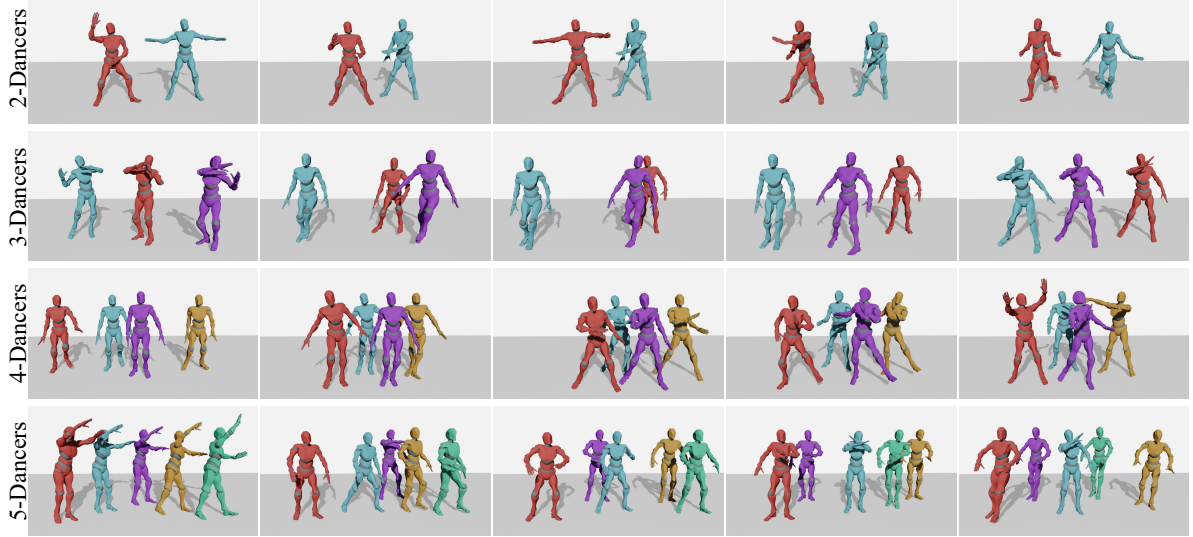


Fig. 6 Results generated by TCDiff++ with different numbers of dancers, demonstrating our adaptability to group sizes.

Table 1 Quantitative comparison with the baselines.

Method	Group-dance Metric			Single-dance Metric			
	GMR↓	GMC↑	TIF↓	FID↓	Div↑	MMC↑	PFC↓
EDGE	63.35	61.72	0.36	31.40	9.57	0.26	2.63
GCD	31.47	80.97	0.17	31.16	10.87	<b>0.26</b>	2.53
CoDancers	26.10	74.05	<b>0.10</b>	<u>23.98</u>	9.48	0.25	3.26
TCDiff	<u>13.86</u>	<u>81.98</u>	<u>0.13</u>	37.47	<u>15.10</u>	0.25	<b>0.51</b>
<b>TCDiff++</b>	<b>10.66</b>	<b>82.00</b>	<b>0.10</b>	<b>21.69</b>	<b>18.48</b>	<u>0.25</u>	<u>1.38</u>

↑ means higher is better, ↓ means lower is better. The best results are highlighted in bold, the second best results are underlined.

features, thus resolving dancer ambiguity while yielding more coherent position-body movements. **Varying Number Analysis.** Figure 6 demonstrates the capability of TCDiff++ to generate high-quality dance motions across a range of group sizes. Our model not only preserves the realism and smoothness of individual motions but also effectively captures group-level dynamics and interactions. In the 5-dancer case, it produces well-balanced and visually harmonious formations. In smaller groups, such as 3 dancers, it generates meaningful interactions like positional swaps, while in the 2- and 4-dancer settings, it exhibits rich motion diversity and coordination patterns. These results highlight the model’s adaptability to varying group sizes and its ability to synthesize coherent choreography that reflects both individual expressiveness and collective structure. More visualization examples can be found on our [page](#).

**Long-duration scenario comparison.** We present a visual comparison of the baseline’s long-duration generation (720 frames) in Figure 7, to better illustrate the superiority of TCDiff++ in this scenario. To better illustrate the dancer formations, we visualize not only the dancers’ pose skeletons but also their positional trajectories, providing a more comprehensive representation of the dynamic formation transitions. Due to the influence of dancer swap phenomena, methods that adopt naive long diffusion sampling (EDGE, GCD) produce severe abrupt swapping during long-duration generation. This is because, during the sampling phase, the lack of spatial information leads to inconsistent dancer position generation across different epochs, causing abrupt swapping when merging the generated segments. Since CoDancers generates one dancer at a time, it lacks inter-dancer information, such as positions. As a result, CoDancers produces unreasonable initial positions due to incomplete group information, resulting in severe overlaps. Moreover, the dancers tend to perform nearly identical movements with minimal interaction, losing the collaborative dynamics that distinguish group dance from solo performances. TCDiff generates dancer positions without considering their movements, which makes it prone to introducing erroneous position estimates due to uncertainty. These errors accumulate significantly during long-duration group dance generation, causing the



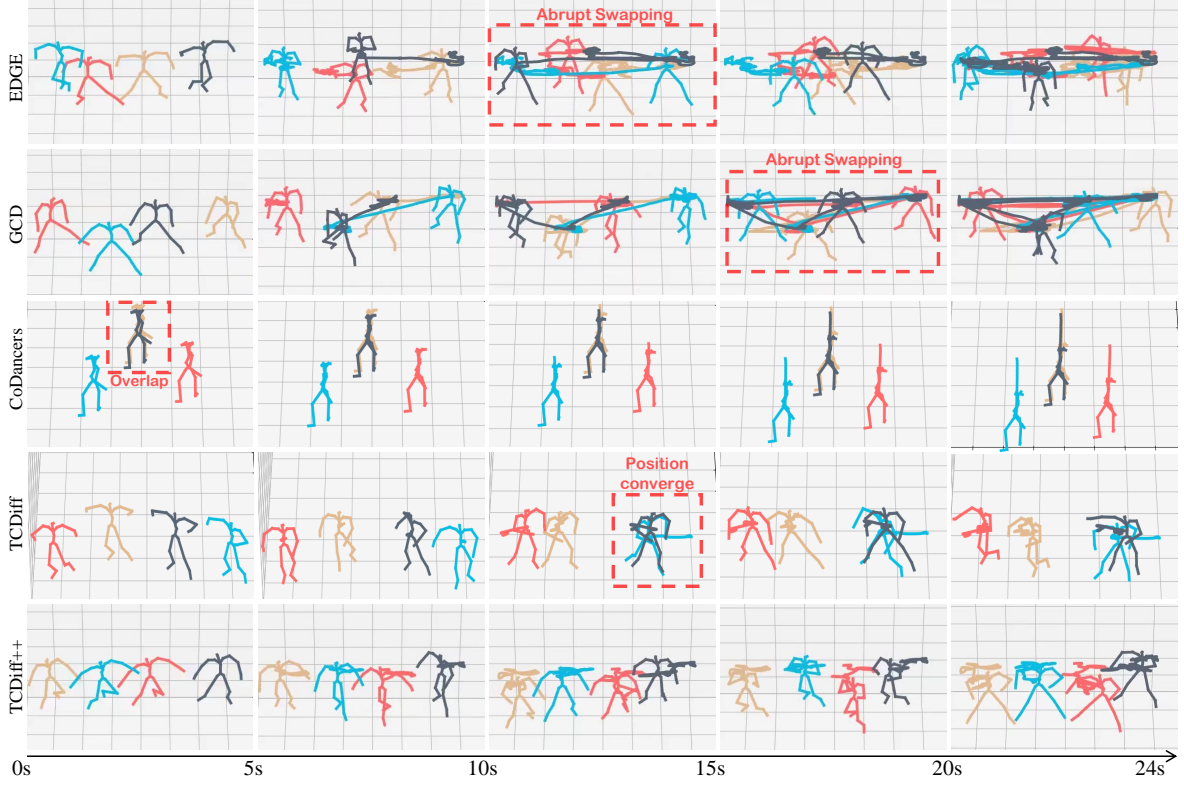


**Fig. 7** Baseline comparison with positional trajectory visualization in a long-duration setting.

dancer coordinates to gradually converge, ultimately resulting in collisions and rendering TCDiff unsuitable for extended sequences. In contrast, the end-to-end TCDiff++ takes into account previously generated results during expansion, improving position consistency across epochs. This effectively reduces the occurrence of abrupt swapping phenomena.

### 5.3 Quantitative Comparison

**Baseline comparison.** Tables 1 and 2 compare our model’s performance with baseline methods. The single-dancer model EDGE struggles in multi-person scenarios, exhibiting severe foot sliding and frequent multi-dancer collisions (high TIF and PFC) due to dancer ambiguity. Similarly, GCD excessively focuses on inter-dancer interaction while neglecting the modeling of coordinate differences between dancers, making it susceptible to dancer ambiguity and resulting in severe foot sliding (high PFC). CoDancers (Yang et al, 2024) reduces ambiguity (low TIF) but compromises inter-dancer correlations (low GMC) and

formation integrity, resulting in discordant group formations, as shown in our user study (Figure 8). Additionally, CoDancers overlooks the relationship between footwork and motion, limiting its ability to align footwork actions with positional changes, which hinders the generation of accurate footwork (low PFC). By decoupling dancer coordinates and movements into two stages, our previous version, TCDiff, mitigates ambiguity, improves coordination, and enhances formation quality. However, this two-stage generation process decouples position trajectory from body modeling, resulting in disjointed actions and displacements, which compromise individual fidelity (FID) and lead to suboptimal results. In contrast, TCDiff++ adopts an end-to-end architecture to mitigate disjoint generation, leveraging its internal module design to resolve dancer ambiguity. This enables more coherent positioning and body movements, leading to consistent superiority in group dance metrics and exceptional performance in Div and FID for single-dance metrics.

**User study** Our user study results are shown in Figure 8. The results show that the visual effects



**Table 2** Quantitative comparison with the baselines for generating 2-5 dancers.

Method	#	GMR↓	GMC↑	TIF↓	FID↓	Div↑	MMC↑
GCD	2	34.09	80.26	0.167	32.62	10.41	0.266
	3	36.25	79.93	0.184	33.94	10.02	0.266
	4	36.28	81.82	0.125	35.89	9.87	0.251
	5	38.43	81.44	0.168	35.08	9.92	0.264
CoDancers	2	24.53	72.88	0.080	26.31	9.01	0.251
	3	27.23	74.34	0.084	24.85	9.15	0.254
	4	26.44	75.34	0.097	25.76	9.43	0.258
	5	26.34	74.22	0.113	25.45	9.77	0.253
TCDiff	2	15.77	81.92	0.121	41.26	16.20	0.263
	3	10.97	81.51	0.123	48.00	19.28	0.253
	4	13.44	81.70	0.149	23.32	10.89	0.253
	5	15.36	82.77	0.109	37.31	14.01	0.236
TCDiff++	2	12.07	82.73	0.058	18.75	14.87	0.249
	3	9.75	81.23	0.098	23.75	22.04	0.251
	4	10.02	82.70	0.143	20.37	15.15	0.252
	5	10.77	81.37	0.106	23.91	21.87	0.266

↑ means higher is better, ↓ means lower is better.

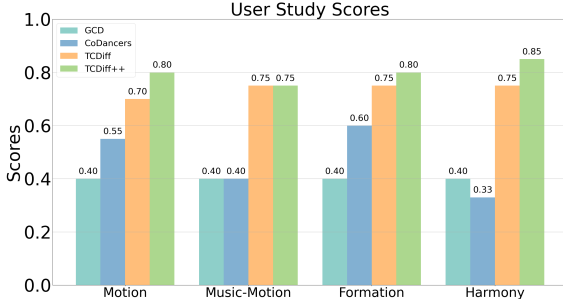


**Fig. 8** User study based on four criteria: motion realism, music-motion correlation, formation aesthetics, and harmony of dancers. Our model has garnered greater user favor, showcasing our superiority in aesthetic appeal.

**Table 3** Baseline comparison in a long-duration setting.

Method	Group-dance Metric				Single-dance Metric		
	GMR↓	GMC↑	TIF↓	FID↓	Div↑	MMC↑	PFC↓
EDGE	67.24	57.65	0.38	35.40	7.97	<b>0.24</b>	3.87
GCD	40.68	79.25	0.28	51.25	7.24	0.20	3.52
CoDancers	35.20	70.53	0.15	43.62	5.48	0.22	4.23
TCDiff	23.87	80.97	0.17	50.47	14.30	0.23	1.87
<b>TCDiff++</b>	<b>14.67</b>	<b>81.64</b>	<b>0.15</b>	<b>20.37</b>	<b>16.19</b>	0.23	<b>1.53</b>

generated by our model are the most favored by users. This is because TCDiff++ effectively mitigates significant visual flaws such as collisions and foot sliding, while producing more consistent footwork movements and resulting in more harmonious dancer formations.

## Evaluating long-duration scenarios.

To assess long-duration performance, we extend the test to 720 frames and evaluate key metrics (Table 3). It can be observed that all models exhibit varying degrees of performance degradation in long-term generation. This includes issues such as frozen frames (resulting in lower MMC) and abrupt swaps (leading to performance declines in PFC and TIF). Due to dancer swap phenomena, naive long diffusion sampling (EDGE, GCD) causes severe abrupt swapping in long-duration generation, as the absence of spatial information disrupts position consistency across epochs. Among them, due to primarily focuses on individual dancers, EDGE maintains more stable motion quality (MMC). However, this comes at the cost of overlooking global feature, leading to more severe dancer collisions (higher TIF) and poor group dance performance. Both CoDancers and the first stage of TCDiff adopt an autoregressive approach, where TCDiff generates trajectory coordinates, while CoDancers synthesize complete dance motions. However, CoDancers solely focuses on individual-level information while neglecting group-level features, leading to degraded performance on group-dance metrics. TCDiff estimates dancer positions without explicitly modeling movements, making it prone to errors from movement uncertainty. These accumulate over time, causing disjointed motions and positional inconsistencies, limiting its suitability for long-duration generation. In contrast, TCDiff++ employs an end-to-end design to improve the coherence between positions and body movements, achieving the best long-duration performance. It also integrates past results to maintain positional consistency and mitigate abrupt swapping.

## 5.4 Ablation Study

To evaluate the effectiveness of our designed module under the long-duration scenario (720 frames), the results are shown in Table 4. We ranked the performance of different ablated models from worst to best to provide an intuitive ordering of performance improvement. The results show that the model achieves the best performance when all modules are applied simultaneously (Full). Overall, all modules have contributed to improving the model’s performance on group metrics, thereby

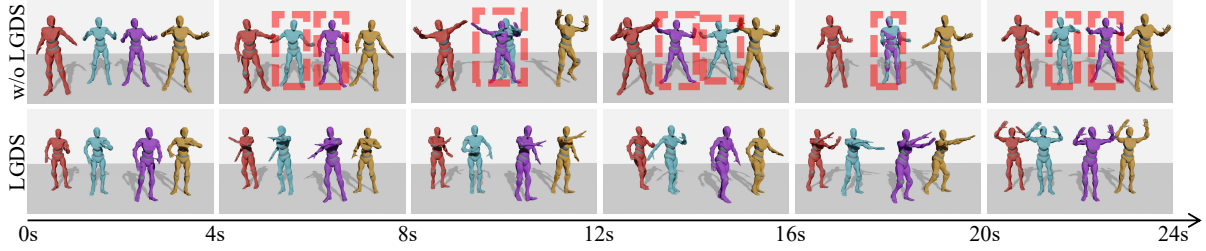


**Fig. 9** Comparison of group dance generation results with and without the LGDS module under long-duration conditions. LGDS effectively reduces abrupt dancer swapping in long-term generation, enhancing spatial consistency.

demonstrating their effectiveness in enhancing the harmony of group dance. This improvement is attributed to their varying degrees of mitigation of multi-dancer collisions and foot sliding, leading to more realistic dance movements. Notably, our proposed Fusion Projection (FP) and Long Group Diffusion Sampling (LGDS) significantly reducing abrupt swapping (PFC and TIF), as shown in Figure 9 and 10 enhancing the visual quality of the generated results. Among them, the simple-yet-effective FP module contributes the most to improving the performance of the end-to-end model, effectively mitigating the adverse effects of dancer ambiguity. Meanwhile, the LGDS strategy enhances the model’s performance in extending group dance motion sequences within the diffusion framework in a training-free manner, effectively reducing the occurrence of abrupt swapping. In mitigating foot sliding, the Footwork Adaptor and Swap Mode modules play a significant role by enhancing the model’s ability to capture sequential dependencies and incorporating additional spatial information. In alleviating multi-dancer collision, the Dancer Positioning Loss (DPE) and distance-consistency loss  $\mathcal{L}_D$  are particularly effective, as they amplify feature distinctions among dancers and introduce spatial constraints.

For simplicity, we use the following abbreviations throughout the subsequent sections: Fusion Projection (FP), Footwork Adaptor (FA), Sequence Decoder (SD), Dancer Positioning Embedding (DPE), Swap Mode (SM), Long Group Dance Sampling (LGDS) and  $\mathcal{L}_D$  for distance-consistency loss.

**Effectiveness of FP.** With FP, the model demonstrates significant improvements across both multi-dancer and single-dancer metrics. GMR decreases from 30.75 to 14.67, indicating enhanced group formation quality, while GMC increases from 79.14 to 81.64, reflecting stronger

**Table 4** Ablation study results.

Method	Group-dance Metric			Single-dance Metric			
	GMR↓	GMC↑	TIF↓	FID↓	Div↑	MMC↑	PFC↓
w/o FP	30.75	79.14	0.23	43.69	<b>17.48</b>	0.21	1.89
w/o FA	25.37	80.75	0.15	33.27	12.75	0.22	2.34
w/o SD	25.75	80.72	0.17	28.75	14.24	<b>0.25</b>	<b>1.52</b>
w/o DPE	20.97	80.91	0.18	40.75	10.52	0.23	1.58
w/o SM	16.71	<u>81.60</u>	<u>0.17</u>	25.97	15.75	0.23	1.75
w/o LGDS	<u>15.72</u>	<u>80.34</u>	0.18	36.23	10.52	0.22	1.92
w/o $\mathcal{L}_D$	18.72	80.91	0.18	<u>24.34</u>	15.75	0.23	1.87
Full	<b>14.67</b>	<b>81.64</b>	<b>0.15</b>	<b>20.37</b>	<u>16.19</u>	<u>0.23</u>	<u>1.53</u>

correlation among dancers. Additionally, TIF is reduced from 0.23 to 0.15, suggesting fewer dancer collisions and improved formation organization. With FP, the model reduces random abrupt swapping and unrealistic formations, resulting in more structured and coherent dance generation. This refinement leads to a slight decrease in Div from 17.48 to 16.19, while significantly lowering FID from 43.69 to 20.37, thereby enhancing the realism of the generated dances. Lastly, PFC decreases from 1.89 to 1.53, improving the physical plausibility of footwork. These results confirm that FP plays a crucial role in refining both structural coherence and visual quality in dance generation. Figure 10 illustrates that integrating FP effectively reduces dancer overlap and abrupt swapping. The coordinate trajectories reveal a more reasonable dancer formation, further improving the visual quality of the generated results. This is because FP amplifies the differences between dancers in high-dimensional space, which effectively helps reduce dancer ambiguity.

**Effectiveness of FA.** Our FA markedly enhances the model’s PFC value, and even enhances model’s performance in group dance metrics and FID. Notably, adding FA reduces PFC from 2.34 to 1.53, enhancing the physical plausibility of footwork. With FA, GMR decreases from

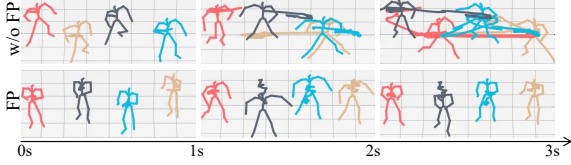


**Fig. 10** Comparison with and without the FP module in our end-to-end TCDiff++. The skeletal motion visualization demonstrates that the FP module effectively mitigates overlap and abrupt swapping phenomena.

25.37 to 14.67, indicating improved group formation quality, while GMC increases from 80.75 to 81.64, enhancing dancer correlation. For single-dancer evaluation, FA significantly reduces FID from 33.27 to 20.37, enhancing the similarity to real dance sequences by ensuring more realistic footwork. Moreover, Div increases from 12.75 to 16.19, indicating greater motion variety. This is because FA captures the connection between positional shifts and footwork, leading to more realistic dance footwork.

**Effectiveness of SD.** For group-dance evaluation, GMR decreases from 25.75 to 14.67, indicating a significant improvement in group formation realism. GMC increases slightly from 80.72 to 81.64, suggesting better dancer coordination. TIF also decreases from 0.17 to 0.15, reflecting fewer dancer collisions. For single-dance evaluation, FID improves from 28.75 to 20.37, indicating better alignment with real dance sequences. Div increases from 14.24 to 16.19, showing more motion variety in the full model. Our SD leverages the SSM architecture to enhance selection in sequential data, therefore it becomes easier to generate movements with rich expressiveness and less susceptible to noise in long-duration scenario. Although the increased variety (Div) introduces some redundant movements that are slightly misaligned with the musical rhythm (lower MMC), it significantly enhances the model’s visual performance, as reflected in the improved group-dance metrics.

**Effectiveness of DPE.** When compared to the full model, the results show several improvements. GMR increases from 20.97 to 14.67, indicating a significant enhancement in group formation realism with the inclusion of DPE. GMC remains stable, with a slight increase from 80.91 to 81.64, reflecting improved coordination among dancers. TIF decreases from 0.18 to 0.15, showing a reduction in dancer collisions. In terms of

single-dance evaluation, FID improves from 40.75 to 20.37, reflecting a better alignment of generated dances with real sequences. Div increases from 10.52 to 16.19, indicating greater motion variety in the full model. MMC remains unchanged at 0.23, indicating consistent synchronization with the music’s rhythm. PFC slightly decreases from 1.58 to 1.53, showing a slight improvement in footwork plausibility. DPE effectively mitigates multi-dancer collisions (lower TIF), as it incorporates the left-right spatial information of dancers, which helps maintain their relative positioning and enhances the overall performance of the model (improved group-dance metrics and FID).

**Effectiveness of SM.** When compared to the full model, with SM, the GMR increases from 16.71 to 14.67, showing an improvement in group formation realism. TIF decreases slightly from 0.17 to 0.15, suggesting fewer dancer collisions. For single-dance evaluation, FID improves from 25.97 to 20.37, indicating better alignment with real dance sequences. Div decreases slightly from 15.75 to 16.19, reflecting a marginal increase in motion variety. PFC decreases slightly from 1.75 to 1.53, reflecting a slight improvement in footwork plausibility. The improvements can be attributed to SM’s role in reducing spatial uncertainty caused by swap actions. By providing the dancers’ start and end positions, SM helps mitigate the uncertainty during spatial changes (e.g., swaps), resulting in better group coherence, more realistic footwork, and enhanced overall performance.

**Effectiveness of LGDS.** LGDS primarily mitigates abrupt swapping during long-duration extension. Although this transient phenomenon has little impact on quantitative metrics due to its short duration, it significantly degrades visual quality. Thus, while LGDS shows less improvement than FP in metrics, it plays a crucial role in enhancing visual perception. LGDS significantly reduces the occurrence of abrupt swapping in long-term generation (lower TIF) and can be applied training-free during the inference stage, leading to a substantial improvement in model performance. This is because LGDS enforces consistency during the input phase, thereby reducing randomness and ensuring cleaner positional information during generation, which in turn minimizes abrupt swaps. Figure 9 demonstrates that the incorporation of LGDS effectively mitigates abrupt

dancer swapping in long-term generation, ensuring greater spatial consistency during sequence extension and significantly enhancing the visual coherence of group dance.

**Effectiveness of  $\mathcal{L}_D$ .** By emphasizing proper spatial relationships,  $\mathcal{L}_D$  helps maintain optimal distances between dancers. This results in more natural and coherent group formations. Consequently, the model achieves better overall performance in group-dance metrics.

## 6 Conclusion

This paper presents TCDiff++, an innovative framework for generating harmonious group dance through a music-driven, end-to-end approach. We address key challenges in group dance generation, including multi-dancer collisions, single-dancer foot sliding, and long-duration generation. By incorporating dancer positioning embeddings and distance-consistency loss, we effectively reduce collisions and maintain relative positioning. The introduction of swap mode embedding and the Footwork Adaptor minimizes foot sliding, enhancing the quality of individual dancer motions. Furthermore, our long group diffusion sampling strategy, along with the Sequence Decoder layer, ensures smooth and consistent long-duration generation. Experimental results demonstrate that TCDiff++ outperforms existing methods, offering significant improvements in handling long-duration group dance generation while preserving both individual and collective motion quality.

## Declarations

**Competing interests.** The authors declare that they have no known competing financial interests or personal relationships that could have appeared to influence the work reported in this paper.

**Data availability.** This work does not propose any new dataset. The dataset (Le et al, 2023b) that support the findings of this study is openly available at the URL: <https://github.com/aioz-ai/AIOZ-GDANCE>.

**Acknowledgments.** This work was supported by the National Science Fund of China under Grant Nos. U24A20330, 62361166670 and 62072242.

## References

- Ahn H, Kim J, Kim K, et al (2020) Generative autoregressive networks for 3d dancing move synthesis from music. *IEEE Robotics and Automation Letters* 5(2):3501–3508
- Alemi O, Françoise J, Pasquier P (2017) Groovenet: Real-time music-driven dance movement generation using artificial neural networks. *networks* 8(17):26
- Alexanderson S, Nagy R, Beskow J, et al (2023) Listen, denoise, action! audio-driven motion synthesis with diffusion models. *ACM Transactions on Graphics (TOG)* 42(4):1–20
- Artemyeva G, Moshenska T (2018) Role and importance of choreography in gymnastic and dance sports. *Slobozhanskyi herald of science and sport* (4 (66)):27–30
- Bar-Tal O, Chefer H, Tov O, et al (2024) Lumiere: A space-time diffusion model for video generation. In: *SIGGRAPH Asia 2024 Conference Papers*, pp 1–11
- Dabral R, Mughal MH, Golyanik V, et al (2023) Mofusion: A framework for denoising-diffusion-based motion synthesis. In: *Proceedings of the IEEE/CVF conference on computer vision and pattern recognition*, pp 9760–9770
- Dai Y, Zhu W, Li R, et al (2025) Harmonious group choreography with trajectory-controllable diffusion. In: *AAAI*
- Dao T, Gu A (2024) Transformers are SSMS: Generalized models and efficient algorithms through structured state space duality. In: *International Conference on Machine Learning (ICML)*
- Fan R, Xu S, Geng W (2011) Example-based automatic music-driven conventional dance motion synthesis. *IEEE transactions on visualization and computer graphics* 18(3):501–515
- Goodfellow I, Pouget-Abadie J, Mirza M, et al (2020) Generative adversarial networks. *Communications of the ACM* 63(11):139–144

- Gu A, Dao T (2023) Mamba: Linear-time sequence modeling with selective state spaces. arXiv preprint arXiv:231200752
- Gu A, Goel K, Ré C (2022a) Efficiently modeling long sequences with structured state spaces. In: The International Conference on Learning Representations (ICLR)
- Gu T, Chen G, Li J, et al (2022b) Stochastic trajectory prediction via motion indeterminacy diffusion. In: Proceedings of the IEEE/CVF Conference on Computer Vision and Pattern Recognition, pp 17113–17122
- Han B, Ren Y, Peng H, et al (2023) Enchantdance: Unveiling the potential of music-driven dance movement. arXiv preprint arXiv:231215946
- Heusel M, Ramsauer H, Unterthiner T, et al (2017) Gans trained by a two time-scale update rule converge to a local nash equilibrium. *Advances in neural information processing systems* 30
- Ho J, Jain A, Abbeel P (2020a) Denoising diffusion probabilistic models. *Advances in neural information processing systems* 33:6840–6851
- Ho J, Jain A, Abbeel P (2020b) Denoising diffusion probabilistic models. *Advances in neural information processing systems* 33:6840–6851
- Huang R, Hu H, Wu W, et al (2020) Dance revolution: Long-term dance generation with music via curriculum learning. arXiv preprint arXiv:200606119
- Joshi M, Chakrabarty S (2021) An extensive review of computational dance automation techniques and applications. *Proceedings of the Royal Society A* 477(2251):20210071
- Kim J, Oh H, Kim S, et al (2022) A brand new dance partner: Music-conditioned pluralistic dancing controlled by multiple dance genres. In: Proceedings of the IEEE/CVF Conference on Computer Vision and Pattern Recognition, pp 3490–3500
- Kingma DP (2013) Auto-encoding variational bayes. arXiv preprint arXiv:13126114
- Kovar L, Gleicher M (2002) Pighin Frédéric. Motion graphs *ACM T Graphic SIGGRAPH* 2002:473–482
- Le N, Do T, Do K, et al (2023a) Controllable group choreography using contrastive diffusion. *ACM Transactions on Graphics (TOG)* 42(6):1–14
- Le N, Pham T, Do T, et al (2023b) Music-driven group choreography. In: Proceedings of the IEEE/CVF Conference on Computer Vision and Pattern Recognition, pp 8673–8682
- Le N, Do K, Bui X, et al (2024) Scalable group choreography via variational phase manifold learning. In: European Conference on Computer Vision, Springer, pp 293–311
- Lee HY, Yang X, Liu MY, et al (2019) Dancing to music. *Advances in neural information processing systems* 32
- Lee LH, Lin Z, Hu R, et al (2021) When creators meet the metaverse: A survey on computational arts. arXiv preprint arXiv:211113486
- Lee M, Lee K, Park J (2013) Music similarity-based approach to generating dance motion sequence. *Multimedia tools and applications* 62:895–912
- Li H, Li Y, Yang Y, et al (2024a) Dispose: Disentangling pose guidance for controllable human image animation. arXiv preprint arXiv:241209349
- Li J, Zhang Z, Yang J (2024b) Tp2o: Creative text pair-to-object generation using balance swap-sampling. In: European Conference on Computer Vision, Springer, pp 92–111
- Li R, Yang S, Ross DA, et al (2021) Ai choreographer: Music conditioned 3d dance generation with aist++. In: Proceedings of the IEEE/CVF International Conference on Computer Vision, pp 13401–13412
- Li R, Zhao J, Zhang Y, et al (2023) Finedance: A fine-grained choreography dataset for 3d full body dance generation. In: Proceedings of the



- IEEE/CVF International Conference on Computer Vision, pp 10234–10243
- Li R, Dai Y, Zhang Y, et al (2024c) Exploring multi-modal control in music-driven dance generation. arXiv preprint arXiv:240101382
- Li R, Zhang H, Zhang Y, et al (2024d) Lodge++: High-quality and long dance generation with vivid choreography patterns. arXiv preprint arXiv:241020389
- Li R, Zhang Y, Zhang Y, et al (2024e) Lodge: A coarse to fine diffusion network for long dance generation guided by the characteristic dance primitives. In: Proceedings of the IEEE/CVF Conference on Computer Vision and Pattern Recognition, pp 1524–1534
- Liang H, Zhang W, Li W, et al (2024) Intergen: Diffusion-based multi-human motion generation under complex interactions. International Journal of Computer Vision pp 1–21
- Loper M, Mahmood N, Romero J, et al (2023) Smpl: A skinned multi-person linear model. In: Seminal Graphics Papers: Pushing the Boundaries, Volume 2. p 851–866
- Luo S, Hu W (2021) Diffusion probabilistic models for 3d point cloud generation. In: Proceedings of the IEEE/CVF Conference on Computer Vision and Pattern Recognition, pp 2837–2845
- Ma X, Su J, Wang C, et al (2023) 3d human mesh estimation from virtual markers. In: Proceedings of the IEEE/CVF Conference on Computer Vision and Pattern Recognition, pp 534–543
- McFee B, Raffel C, Liang D, et al (2015) librosa: Audio and music signal analysis in python. In: Proceedings of the 14th python in science conference, pp 18–25
- Ofli F, Erzin E, Yemez Y, et al (2011) Learn2dance: Learning statistical music-to-dance mappings for choreography synthesis. IEEE Transactions on Multimedia 14(3):747–759
- Perez E, Strub F, De Vries H, et al (2018) Film: Visual reasoning with a general conditioning layer. In: Proceedings of the AAAI conference on artificial intelligence
- Ren Z, Huang S, Li X (2025) Realistic human motion generation with cross-diffusion models. In: European Conference on Computer Vision, Springer, pp 345–362
- Schwartz JL (1998) The passacaille in lully’s “armide”: Phrase structure in the choreography and the music. Early Music 26(2):301–320
- Siyao L, Yu W, Gu T, et al (2022) Bailando: 3d dance generation by actor-critic gpt with choreographic memory. In: Proceedings of the IEEE/CVF Conference on Computer Vision and Pattern Recognition, pp 11050–11059
- Sohl-Dickstein J, Weiss E, Maheswaranathan N, et al (2015) Deep unsupervised learning using nonequilibrium thermodynamics. In: International conference on machine learning, PMLR, pp 2256–2265
- Song J, Meng C, Ermon S (2020) Denoising diffusion implicit models. arXiv preprint arXiv:201002502
- Tseng J, Castellon R, Liu K (2023a) Edge: Editable dance generation from music. In: Proceedings of the IEEE/CVF Conference on Computer Vision and Pattern Recognition, pp 448–458
- Tseng J, Castellon R, Liu K (2023b) Edge: Editable dance generation from music. In: Proceedings of the IEEE/CVF Conference on Computer Vision and Pattern Recognition, pp 448–458
- Valle-Pérez G, Henter GE, Beskow J, et al (2021) Transflower: probabilistic autoregressive dance generation with multimodal attention. ACM Transactions on Graphics (TOG) 40(6):1–14
- Wang Z, Wang J, Lin D, et al (2023) Intercontrol: Generate human motion interactions by controlling every joint. arXiv preprint arXiv:231115864
- Weng J, Yan Z, Tai Y, et al (2024) Mamballie: Implicit retinex-aware low light enhancement with global-then-local state space. NeurIPS

2024

- Wu S, Lin Y, Zhang F, et al (2024) Direct3d: Scalable image-to-3d generation via 3d latent diffusion transformer. *Advances in Neural Information Processing Systems* 37:121859–121881
- Xiong Z, dong Zhang Z, Chen Z, et al (2024) Novel object synthesis via adaptive text-image harmony. In: *The Thirty-eighth Annual Conference on Neural Information Processing Systems*, URL <https://openreview.net/forum?id=ENLsNDfys0>
- Xue H, Luo X, Hu Z, et al (2024) Human motion video generation: A survey. *Authorea Preprints*
- Yalta N, Watanabe S, Nakadai K, et al (2019) Weakly-supervised deep recurrent neural networks for basic dance step generation. In: *2019 International Joint Conference on Neural Networks (IJCNN)*, IEEE, pp 1–8
- Yang K, Tang X, Diao R, et al (2024) Codancers: Music-driven coherent group dance generation with choreographic unit. In: *Proceedings of the 2024 International Conference on Multimedia Retrieval*. Association for Computing Machinery, New York, NY, USA, ICMR '24, p 675–683, <https://doi.org/10.1145/3652583.3657998>, URL <https://doi.org/10.1145/3652583.3657998>
- Yang S, Yang Z, Wang Z (2023) Longdancediff: Long-term dance generation with conditional diffusion model. *arXiv preprint arXiv:230811945*
- Yao S, Sun M, Li B, et al (2023) Dance with you: The diversity controllable dancer generation via diffusion models. In: *Proceedings of the 31st ACM International Conference on Multimedia*, pp 8504–8514
- Zanfir M, Zanfir A, Bazavan EG, et al (2021) Thundr: Transformer-based 3d human reconstruction with markers. In: *Proceedings of the IEEE/CVF International Conference on Computer Vision*, pp 12971–12980
- Zhang M, Jin D, Gu C, et al (2024) Large motion model for unified multi-modal motion generation. In: *European Conference on Computer Vision*, Springer, pp 397–421
- Zhang S, Zhang Y, Bogo F, et al (2021a) Learning motion priors for 4d human body capture in 3d scenes. In: *Proceedings of the IEEE/CVF International Conference on Computer Vision*, pp 11343–11353
- Zhang Y, Black MJ, Tang S (2021b) We are more than our joints: Predicting how 3d bodies move. In: *Proceedings of the IEEE/CVF Conference on Computer Vision and Pattern Recognition*, pp 3372–3382
- Zhang Y, Zhang H, Hu L, et al (2023) Real-time monocular full-body capture in world space via sequential proxy-to-motion learning. *arXiv preprint arXiv:230701200*
- Zhou Y, Barnes C, Lu J, et al (2019) On the continuity of rotation representations in neural networks. In: *Proceedings of the IEEE/CVF Conference on Computer Vision and Pattern Recognition*, pp 5745–5753
- Zhou Y, Tan G, Li M, et al (2023) Learning from easy to hard pairs: Multi-step reasoning network for human-object interaction detection. In: *Proceedings of the 31st ACM International Conference on Multimedia*, pp 4368–4377
- Zhou Y, Liu L, Gou C (2024) Learning from observer gaze: Zero-shot attention prediction oriented by human-object interaction recognition. In: *Proceedings of the IEEE/CVF Conference on Computer Vision and Pattern Recognition*, pp 28390–28400
- Zhou Z, Wang B (2023) Ude: A unified driving engine for human motion generation. In: *Proceedings of the IEEE/CVF Conference on Computer Vision and Pattern Recognition*, pp 5632–5641
- Zhu S, Chen JL, Dai Z, et al (2024) Champ: Controllable and consistent human image animation with 3d parametric guidance. In: *European Conference on Computer Vision*, Springer, pp 145–162